Molecular Plant Pathology

MOLECULAR PLANT PATHOLOGY (2017) 18(3), 323–335 DOI: 10.1111/mpp.12399

The role of a cytosolic superoxide dismutase in barley–pathogen interactions

DAMIEN J. LIGHTFOOT[1]†, GRAHAM R. D. MCGRANN[2]‡ AND AMANDA J. ABLE[1,*]

[1]School of Agriculture, Food and Wine, The University of Adelaide, Waite Research Institute, PMB 1, Glen Osmond, SA 5064, Australia
[2]Department of Crop Genetics, John Innes Centre, Norwich NR4 7UH, UK

SUMMARY

Reactive oxygen species (ROS), including superoxide ($O_2^{\cdot-}/HO_2^{\cdot}$) and hydrogen peroxide (H_2O_2), are differentially produced during resistance responses to biotrophic pathogens and during susceptible responses to necrotrophic and hemi-biotrophic pathogens. Superoxide dismutase (SOD) is responsible for the catalysis of the dismutation of $O_2^{\cdot-}/HO_2^{\cdot}$ to H_2O_2, regulating the redox status of plant cells. Increased SOD activity has been correlated previously with resistance in barley to the hemi-biotrophic pathogen *Pyrenophora teres* f. *teres* (*Ptt*, the causal agent of the net form of net blotch disease), but the role of individual isoforms of SOD has not been studied. A cytosolic CuZnSOD, *HvCSD1*, was isolated from barley and characterized as being expressed in tissue from different developmental stages. *HvCSD1* was up-regulated during the interaction with *Ptt* and to a greater extent during the resistance response. Net blotch disease symptoms and fungal growth were not as pronounced in transgenic *HvCSD1* knockdown lines in a susceptible background (cv. Golden Promise), when compared with wild-type plants, suggesting that cytosolic $O_2^{\cdot-}/HO_2^{\cdot}$ contributes to the signalling required to induce a defence response to *Ptt*. There was no effect of *HvCSD1* knockdown on infection by the hemi-biotrophic rice blast pathogen *Magnaporthe oryzae* or the biotrophic powdery mildew pathogen *Blumeria graminis* f. sp. *hordei*, but *HvCSD1* also played a role in the regulation of lesion development by methyl viologen. Together, these results suggest that HvCSD1 could be important in the maintenance of the cytosolic redox status and in the differential regulation of responses to pathogens with different lifestyles.

Keywords: hemi-biotroph, net blotch disease, plant–pathogen interaction, reactive oxygen species, superoxide dismutase.

*Correspondence: Email: amanda.able@adelaide.edu.au
†Present address: Biological and Environmental Sciences & Engineering Division, King Abdullah University of Science and Technology, Thuwal, 23955-6900 Saudi Arabia
‡Present address: Crop Protection Team, Crop and Soil Systems Group, SRUC, Edinburgh EH9 3JG, UK

INTRODUCTION

Reactive oxygen species (ROS), including singlet oxygen ($^1O_2$), hydroxyl radical ($OH^{\cdot}$), superoxide ($O_2^{\cdot-}/HO_2^{\cdot}$) and hydrogen peroxide (H_2O_2), are toxic by-products of metabolism, potentially harmful to plant cell integrity (Dat *et al.*, 2002; Mittler *et al.*, 2004; Sutherland, 1991). However, ROS, together with nitric oxide (NO), have been shown to be essential for signalling processes during metabolism and development, as well as during responses to abiotic and biotic stress (Baxter *et al.*, 2014; Groß *et al.*, 2013; Lehmann *et al.*, 2015). On recognition of a pathogen, a rapid oxidative burst can occur in the plant under attack and ROS production appears to be necessary for further plant defence reactions (Heller and Tudzynski, 2011; Lehmann *et al.*, 2015; O'Brien *et al.*, 2012), such as the hypersensitive response (HR) (Gadjev *et al.*, 2008).

$O_2^{\cdot-}/HO_2^{\cdot}$, H_2O_2 and NO have been shown to be essential for the HR in various plant–pathogen interactions in which the pathogen is known to be primarily biotrophic during its life cycle (Able *et al.*, 1998, 2000; Delledonne *et al.*, 2001; Levine *et al.*, 1994). Tissue death resulting from ROS-induced HR impedes successful infection by biotrophs, leading to host resistance. However, the HR might increase host susceptibility to necrotrophic pathogens providing dead tissue for nutritional purposes (Able, 2003; Barna *et al.*, 2012). Indeed, ROS have been shown to be produced to a greater extent during susceptible plant responses to fungi with necrotrophic stages in their life cycles, including in barley infected with *Rhynchosporium secalis* or *Pyrenophora teres* (Able, 2003; Liu *et al.*, 2015), wheat with *Zymoseptoria tritici* (syn. *Septoria tritici*; Shetty *et al.*, 2003) and Arabidopsis with *Botrytis cinerea* (Govrin and Levine, 2000). Necrotrophic pathogens may therefore exploit ROS production by the plant or may even contribute to ROS production to induce cell death, as has been suggested for *B. cinerea* (Govrin and Levine, 2000), *P. teres* (Able, 2003) and *Leptosphaeria maculans* (Li *et al.*, 2008a,b). Removal of *in planta* H_2O_2 by infiltrating wheat leaves with the H_2O_2 scavenger catalase (CAT) during the necrotrophic stage of the infection by *Z. tritici* led to susceptibility as a result of enhanced growth of the pathogen, but infiltration with H_2O_2 led to decreased growth of the pathogen (Shetty *et al.*, 2007). These authors suggested that the fungus still grows *in planta* in spite of ROS production and therefore may not actually need ROS to be virulent. The

observation that differences in the virulence of *P. teres* isolates were not correlated with their ability to produce ROS supports this suggestion (Able, 2003). In addition, the infiltration of barley leaves with ROS scavengers did not affect the growth of *P. teres in planta*, but the extent of symptom development was partially reduced. Necrosis-inducing toxins produced by many of the pathogens discussed here also contribute to symptom development and possibly virulence (Ismail *et al.*, 2014a; Liu *et al.*, 2015; Sarpeleh *et al.*, 2007, 2008). However, ROS are necessary for the regulation of various fungal processes associated with virulence, including hyphal growth, fusion and branching, and the differentiation of asexual spores, fungal cell walls, fruiting bodies and appressoria (Dirschnabel *et al.*, 2014; Georgiou *et al.*, 2006; Scott and Eaton, 2008; Tudzynski *et al.*, 2012). Given the complex associations between fungal growth rates, toxin production and virulence, the potential involvement of plant-produced ROS and their detoxification requires further study.

During biotic and abiotic stress, the levels of ROS increase as a result of electron leakage from the electron transport chains in chloroplasts and mitochondria (Asada *et al.*, 1974; Pastori and Foyer, 2002; Rhoads *et al.*, 2006). Membrane-bound NADPH oxidases and cell wall peroxidases have also been shown to be the main producers of ROS during plant–pathogen interactions (O'Brien *et al.*, 2012). Elevated ROS levels induce the biosynthesis of non-enzymatic antioxidants, such as ascorbate, polyamines and glutathione (Blokhina *et al.*, 2003; Conklin and Last, 1995), and increase the activity of the antioxidant enzymes superoxide dismutase (SOD), CAT and glutathione-*S*-transferase (GST) (Blokhina *et al.*, 2003; Mittler *et al.*, 2004), especially in cells that surround an HR (Levine *et al.*, 1994). The main ROS produced, $O_2^{\cdot-}/HO_2^{\cdot}$, is usually converted to the less toxic H_2O_2 by SOD. H_2O_2 can be degraded more easily by antioxidants, including CAT and ascorbate peroxidase (APX) (Groß *et al.*, 2013). Given the demonstrated role of H_2O_2 in various plant–pathogen interactions (Able *et al.*, 2000; Delledonne *et al.*, 2001; Hückelhoven *et al.*, 1999; Levine *et al.*, 1994), changes in the levels of SOD may therefore also play a significant role during plant–pathogen interactions (Frederickson Matika and Loake, 2014), especially during the HR (Delledonne *et al.*, 2001).

SODs, which are usually defined by their metal co-factors (Mn, Fe or CuZn), can be found at all sites of $O_2^{\cdot-}/HO_2^{\cdot}$ production (Alscher *et al.*, 2002; Bowler *et al.*, 1994; Miller, 2012). FeSODs are primarily located in the chloroplast in some plants (Van Camp *et al.*, 1990), with three identified in Arabidopsis (Myouga *et al.*, 2008). MnSODs are located in the mitochondria and peroxisomes in an independent manner (del Rio *et al.*, 2003), whereas CuZnSODs are usually located in the chloroplast and the cytosol of plants (Alscher *et al.*, 2002). The cytosolic form of CuZnSOD can also localize to the nucleus (Ogawa *et al.*, 1996). Sequences for the cytosolic and chloroplastic forms of CuZnSOD are easily distinguishable because of differences in the numbers and positions of introns (Kliebenstein *et al.*, 1998).

We have shown previously that total SOD activity increases significantly during resistant interactions between barley and *P. teres* f. *teres* (*Ptt*) when compared with the susceptible response (Able, 2003). Furthermore, a suppressive subtractive hybridization (SSH) screen identified a 181-bp fragment up-regulated during the resistance response and with similarity to CuZnSOD (Bogacki *et al.*, 2008). These results, together with previous observations that $O_2^{\cdot-}/HO_2^{\cdot}$ is produced during the susceptible response (Able, 2003), suggest that the removal of $O_2^{\cdot-}/HO_2^{\cdot}$ might be important during the resistance response to *Ptt*, a pathogen with a necrotrophic stage in its life cycle (Lightfoot and Able, 2010). Here, we report the subsequent identification and characterization of the up-regulated CuZnSOD as *HvCSD1*. Using RNA interference (RNAi) knockdown lines, we have also functionally analysed *HvCSD1* for its potential role in ROS-induced lesion formation and during the interaction between barley and *Ptt*, as well as another hemi-biotroph *Magnaporthe oryzae* and the obligate biotroph *Blumeria graminis* f. sp. *hordei* (*Bgh*).

RESULTS

Identification and characterization of *HvCSD1*

A partial barley cDNA with high sequence homology to the rice CuZnSOD, *OsSODCc1*, has been identified previously using SSH (Bogacki *et al.*, 2008). Subsequently, a full-length cDNA clone with 3′ and 5′ untranslated regions (UTRs) (799 nucleotides) was isolated (Fig. 1a). The deduced amino acid sequence for the open reading frame (152 amino acid residues) contains the conserved copper-binding [histidine-45 (His-45), His-47, His-62, His-119], zinc-binding [His-62, His-70, His-79, aspartic acid-82 (Asp-82)] and conserved cysteine (Cys-56 and Cys-145) residues common in CuZnSOD proteins. The lack of a signal peptide suggested that the protein is cytosolic, and phylogenetic analysis grouped the clone with cytoplasmic CuZnSODs, such as *AtCSD1* (Fig. 1b). Phylogenetic analysis clearly separated cytoplasmic, peroxisomic and chloroplastic SODs. The exon structure of the genomic DNA of the clone also suggested that the protein was cytosolic (Table S1, see Supporting Information). The seven exons are of the same length as for other cytosolic CuZnSODs, including *AtCuZn Superoxide Dismutase 1*. Hence, we have named the gene characterized in this study as *HvCSD1* (Accession number KU179440). The predicted localization to the cytoplasm (and nucleus) was confirmed using 35S::HvCSD1-GFP localization (GFP, green fluorescent protein) (Fig. 1c).

Semi-quantitative reverse transcription-polymerase chain reaction (sqRT-PCR) revealed that the *HvCSD1* gene expression levels are constitutive, regardless of tissue type (Fig. 2). *HvCSD1* gene expression is induced by infection with *Ptt* in both susceptible

(a)

```
  1 gaaaccagcatcatccatcccctcccctccccaagtcagtcataaacccaagtcggactc
 61 gccttcctcctcctcccaaccactccgctcttccgccgcgcatcgcaccgggggtcac
121 ctgagatcacatacacaatggtgaaggctgtagctgtgcttaccggcagcgagggtgtca
                    M  V  K  A  V  A  V  L  T  G  S  E  G  V  K
181 agggcaccatcttcttcacccaggagggagatggcccaaccaccgtgacgggaagtgtca
     G  T  I  F  F  T  Q  E  G  D  G  P  T  T  V  T  G  S  V  T
241 ccggactcaaggaaggcttcacggcttccatgtgcacgctcttggtgacaccaccaacg
     G  L  K  E  G  L  H  G  F  H  V  H  A  L  G  D  T  T  N  G
301 gctgcatgtcaactggaccgcacttcaaccccgctggtcatgtgcatggggcacccgaag
     C  M  S  T  G  P  H  F  N  P  A  G  H  V  H  G  A  P  E  D
361 atgaaatccgccatgctggtgacctcggaaatgtgacagctggagcggatggtgttgcta
     E  I  R  H  A  G  D  L  G  N  V  T  A  G  A  D  G  V  A  N
421 acatcaatgttactgactgccatatccccttgctggaccacattcaatcattggccgtg
     I  N  V  T  D  C  H  I  P  L  A  G  P  H  S  I  I  G  R  A
481 ctgttgtcgtccatggtgatgctgatgatcttggcaagggtggacatgagcttagcaaga
     V  V  V  H  G  D  A  D  D  L  G  K  G  G  H  E  L  S  K  S
541 gcactggaaacgctggggcgcgcgttgcttgcgggatcatcgggctccagggctaagatg
     T  G  N  A  G  A  R  V  A  C  G  I  I  G  L  Q  G  *
601 ccgtcttcgcaggctgatgaaggccgtacagatcttggcacttgaaggacaccgacttgc
661 aattgctatctatttaaataagcacaccatctatgatcgctttttagtgtgcatcattt
721 gtgtcgattcctatgtgaactttcatatcactgtcatttggctttttgagttgcgtgact
781 ggaacagttcagttctgtcaaaaaaaaaaaaaaaaaaaa
```

(b)

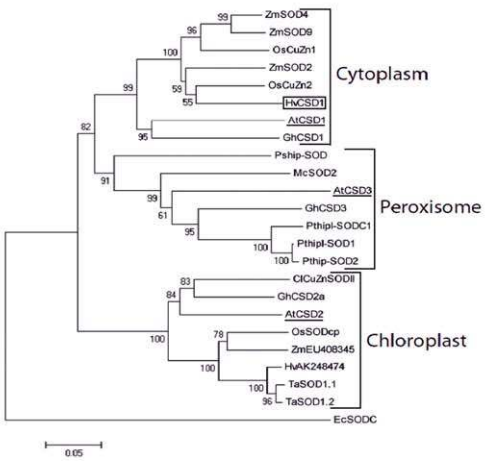

(c)

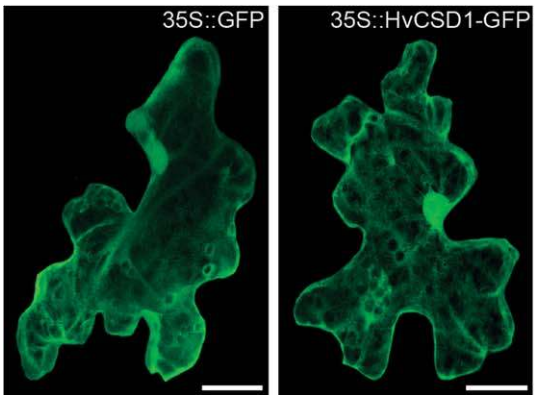

Fig. 1 Characterization of *HvCSD1*. (a) cDNA sequence of *HvCSD1* (Accession number: KU179438; CI9214) and its derived amino acid residues. Conserved copper-binding residues are underlined with a full line, conserved zinc-binding residues are underlined with a broken line and conserved cysteines, which are required for disulfide bond formation, have â underneath them. (b) Comparison of *HvCSD1* (boxed) with known and predicted nucleotide sequences for copper–zinc superoxide dismutases (CuZnSODs) in other species, including cytoplasmic, peroxisomic and chloroplastic *CSD* genes from *Arabidopsis thaliana* (underlined). Branch lengths (bar) infer evolutionary distances at 0.05 substitutions per site. Accession numbers are listed in 'Experimental procedures'. The species are indicated as follows: At, *Arabidopsis thaliana*; Cl, *Citrullus lanatus*; Ec, *Escherichia coli*; Gh, *Gossypium hirsutum*; Hv, *Hordeum vulgare*; Mc, *Mesembryanthemum crystallinum*; Os, *Oryza sativa*; Pship, *Pinus sylvestris* high isoelectric point; Pthip, *Populus trichocarpa* high isoelectric point; Ta, *Triticum aestivum*; Zm, *Zea mays*. (c) Transient expression of 35S::GFP and 35S::HvCSD1-GFP in epidermal cells of *Nicotiana benthamiana* leaves. Cells were analysed 3 days after infiltration with *Agrobacterium tumefaciens* containing the appropriate vector. Composite images (*Z*-step stacks collected using confocal microscopy) are representative of three independent experiments. Bar, 25 μm. GFP, green fluorescent protein.

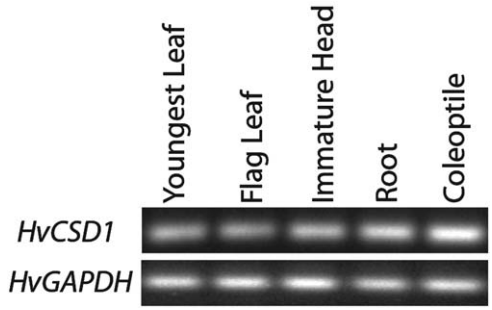

Fig. 2 Expression of *HvCSD1* transcript in different tissues. Spatial expression of *HvCSD1* was analysed by semi-quantitative reverse transcription-polymerase chain reaction (sqRT-PCR) using gene-specific primers and 30 amplification cycles. *Glyceraldehyde 3-phosphate dehydrogenase* (*HvGAPDH*) was used as an internal control. Images shown are representative of three independent experiments for three biological replicates.

(Sloop) and resistant (CI9214) cultivars (Fig. 3). The increase in *HvCSD1* expression was greater in the incompatible interaction between CI9214 and *Ptt* and occurred more quickly than in the compatible interaction between Sloop and *Ptt*. *HvCSD1* expression was greater from 18 h post-inoculation (hpi) in the resistant cultivar compared with the susceptible cultivar (Fig. 3), regardless of the lower expression of the internal control gene *HvGAPDH* in the infected resistant cultivar.

Development of transgenic *HvCSD1* RNAi knockdown barley lines

Based on the expression pattern of *HvCSD1* in response to *Ptt* in both resistant and susceptible interactions, transgenic RNAi-silencing knockdown lines for *HvCSD1* were generated to assess gene function during disease development. Two T_2 homozygous transgenic lines, HvCSD1-RNAi1 and HvCSD1-RNAi2, were produced from two independent transformation events and contained a single copy of the gene (Fig. S1, see Supporting Information). The extent of *HvCSD1* knockdown was confirmed using RNA

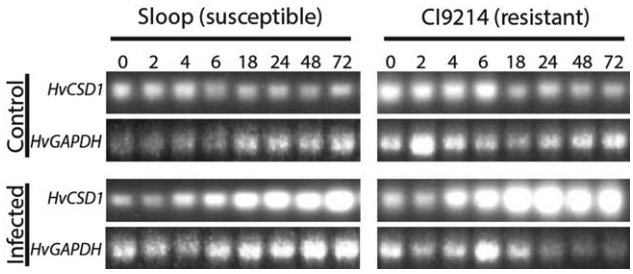

Fig. 3 Temporal expression of *HvCSD1* during the interaction between barley and *Pyrenophora teres* f. *teres* (*Ptt*). Transcript levels of *HvCSD1* were monitored in the susceptible barley cv. Sloop and the resistant barley breeding line CI9214 at 0, 2, 4, 6, 18, 24, 48 and 72 h post-inoculation with conidia from *Ptt* (Infected) or sterile nanopure water (Control). Material derived from the leaves was analysed by semi-quantitative reverse transcription-polymerase chain reaction (sqRT-PCR) using gene-specific primers and 30 amplification cycles. *Glyceraldehyde 3-phosphate dehydrogenase* (*HvGAPDH*) was used as an internal control. Images shown are representative of three independent experiments for three biological replicates.

expression analysis (Fig. S2a, b, see Supporting Information). sqRT-PCR analysis indicated that both HvCSD1-RNAi1 and HvCSD1-RNAi2 had lower levels of *HvCSD1* transcript than the wild-type cv. Golden Promise. Of the two lines, HvCSD1-RNAi1 appeared to have lower levels of the *HvCSD1* transcript (Fig. S2a). qRT-PCR analysis of *HvCSD1* levels in HvCSD1-RNAi indicated that the target transcript levels were knocked down to approximately 20% of the wild-type level (Fig. S2b). Assay of SOD activity also confirmed that the CuZnSOD activity was lower in both transgenic lines compared with wild-type cv. Golden Promise (Fig. S2c).

Disease development on *HvCSD1* RNAi lines

When *HvCSD1* was silenced, the development of disease symptoms during a compatible interaction with *Ptt* was significantly reduced (Fig. 4; $P < 0.05$). The percentage of leaf area affected by necrosis and chlorosis was significantly reduced by 168 hpi in the RNAi lines (Fig. 4a, b; $P < 0.05$), as was fungal development (Fig. 4c; $P < 0.05$). At 120 hpi, fungal development was significantly lower for the resistant breeding line CI9214 and both RNAi lines ($P < 0.05$). However, after 120 hpi, fungal development proceeded further in the resistant breeding line CI9214 than in either of the knockdown lines (Fig. 4c; $P < 0.05$), but did not reach the levels observed in the susceptible cv. Golden Promise. By 168 hpi, the leaves in the compatible interaction had collapsed (data not shown), the fungus was sporulating and its hyphae had spread throughout the entire tissue [a score of 9–10 on the fungal development scale of Lightfoot and Able (2010)]. In comparison, the fungal hyphae had only just started to penetrate into the mesophyll in the *HvCSD1* knockdown lines and only some cell death was evident near the hyphae (a fungal development score of 6–7).

Irrespective of RNAi silencing, *HvCSD1* gene expression was induced by *Ptt* in both transgenic lines (Fig. 4d). Increases in *HvCSD1* transcript levels were greatest in the resistant breeding line CI9214. *HvCSD1* transcript levels were induced in the knockdown lines to a slightly greater extent than that in the susceptible cv. Golden Promise early in the interaction, peaking at 24 hpi (Fig. 4d). CuZnSOD protein activity was also induced by *Ptt* in CI9214, Golden Promise and HvCSD1-RNAi1 (Fig. 4e). Increases in CuZnSOD activity were greatest by 24 hpi in the resistance response to *Ptt* (in CI9214).

The effect of silencing of *HvCSD1* on the development of disease symptoms during compatible interactions with the hemibiotrophic *M. oryzae* and the obligate biotroph *Bgh* was also examined. No significant differences were observed between the knockdown line HvCSD1-RNAi1 and the wild-type cv. Golden Promise for the development of disease symptoms for either pathogen (Fig. 5a, c). There was no significant effect of *HvCSD1* silencing on the number of lesions formed by the blast fungus *M. oryzae* (Fig. 5b; $P = 0.923$) or the number of colonies formed by the powdery mildew fungus *Bgh* (Fig. 5d; $P = 0.417$).

Effect of *HvCSD1* transcript knockdown on sensitivity to ROS-induced cell death

Whether the silencing of *HvCSD1* affected the sensitivity to ROS-induced lesion formation was also examined. In general, the RNAi line HvCSD1-RNAi1 appeared to exhibit larger lesions caused by the H_2O_2 donor alloxan, the mitochondrial $O_2^{\cdot-}/HO_2^{\cdot}$ donor menadione and the chloroplastic $O_2^{\cdot-}/HO_2^{\cdot}$ donor methyl viologen, compared with the wild-type cv. Golden Promise (Fig. 6a). However, only the observed increase in methyl viologen-induced lesion size was statistically significant between the knockdown line and wild-type plants (Fig. 6b; $P < 0.05$).

DISCUSSION

The role of ROS in resistance responses to biotrophic pathogens is well established (Heller and Tudzynski, 2011; Lehmann *et al.*, 2015). ROS have also been identified during infection by fungi with necrotrophic stages in their life cycle and could possibly contribute to cell death during susceptible responses, such as observed for *P. teres* on barley (Able, 2003; Liu *et al.*, 2015) and

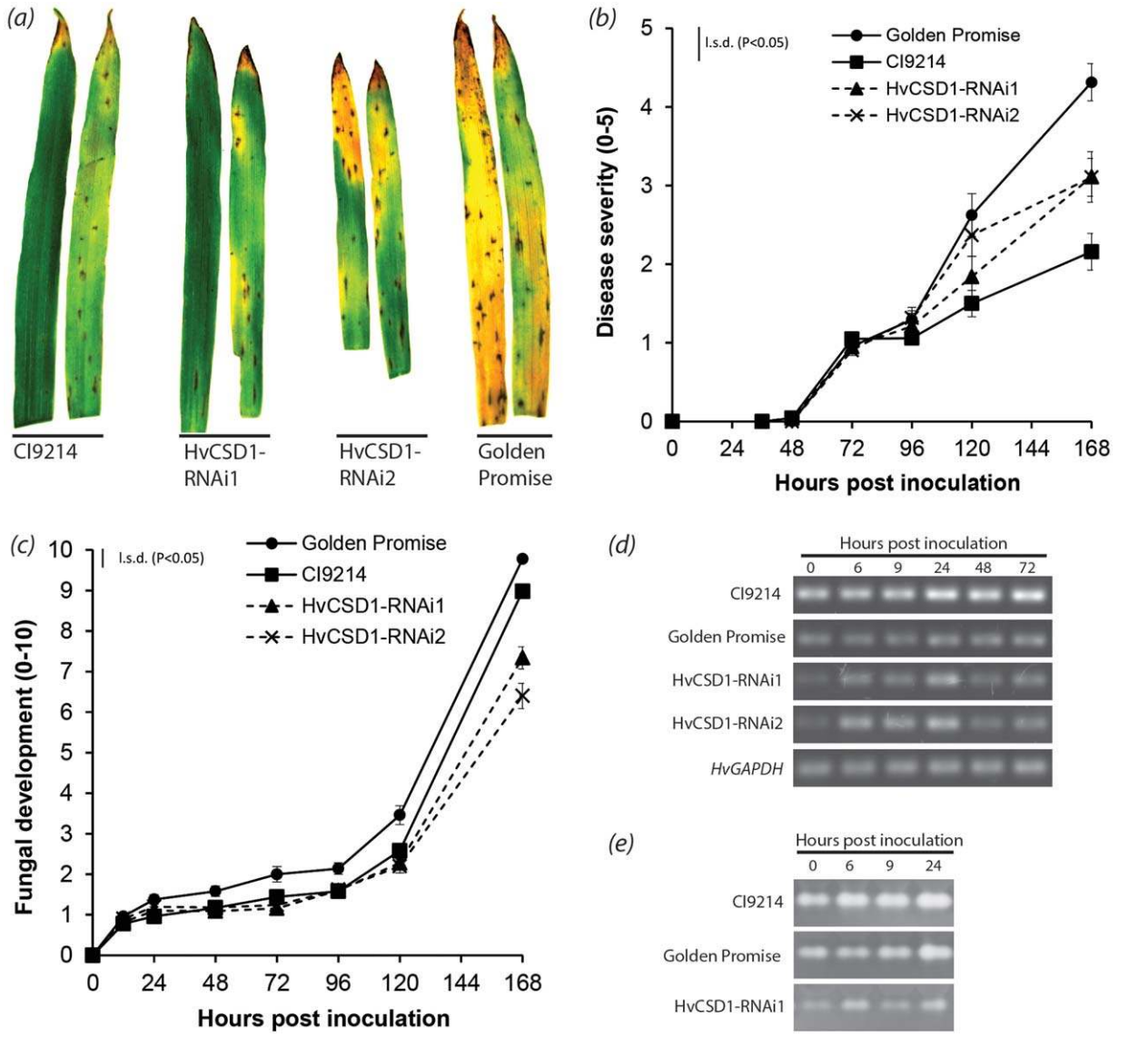

Fig. 4 Effect of *HvCSD1* silencing on the interaction between barley and *Pyrenophora teres* f. *teres* (*Ptt*). (a) Net blotch disease symptoms on the second youngest leaf at 168 h post-inoculation (hpi). Images are representative of two independent experiments with a total of eight leaves. (b) Disease severity was determined for the second youngest leaf of *Ptt*-inoculated barley plants using a scale of 0–5, where '0' represents 0% coverage of the leaf with symptoms (chlorosis and necrosis), '1' represents 1%–10% coverage, '2' represents 11%–25% coverage, '3' represents 26%–50% coverage, '4' represents 51%–75% coverage and '5' represents 76%–100% coverage. No symptoms were observed on mock-inoculated controls. Data shown are means ± standard error (SE) for $n = 21$ across two experiments. The least significant difference (l.s.d.) at $P < 0.05$ is shown for comparisons among treatments at each time point. (c) Fungal development scores using a scale of 0–10, where '0' indicates that conidia are visible but have not germinated and '10' indicates that stromata are mature with conidiophores (Lightfoot and Able, 2010). Ten germinated conidia were assessed on each of five leaves. The data shown are means ± SE for $n = 50$ across two experiments. The l.s.d. at $P < 0.05$ is shown for comparison among treatments at each time point. (d) Temporal expression of *HvCSD1* during the interaction between *Ptt* and barley. *HvCSD1* transcript levels were analysed by semi-quantitative reverse transcription-polymerase chain reaction (sqRT-PCR) using gene-specific primers and 30 amplification cycles. *Glyceraldehyde 3-phosphate dehydrogenase* (*HvGAPDH*) was used as an internal control. Images shown are representative of two independent experiments for four biological replicates. (e) Activity staining for copper–zinc superoxide dismutase (CuZnSOD) following non-denaturing polyacrylamide gel electrophoresis (PAGE) of 100 μg total protein. Images shown are representative of two independent experiments for four biological replicates.

B. cinerea on Arabidopsis (Govrin and Levine, 2000). Although the induction of ROS production has been correlated with susceptibility, ROS is not necessarily correlated with the ability of the pathogen to grow *in planta* (Able, 2003; Shetty *et al.*, 2007). Various virulence-associated toxins and/or effectors, usually produced during the later stages of necrotrophic interactions, can also contribute to cell death, fungal growth, disease symptoms and the suppression of defence responses (Lo Presti *et al.*, 2015). *Ptt* not

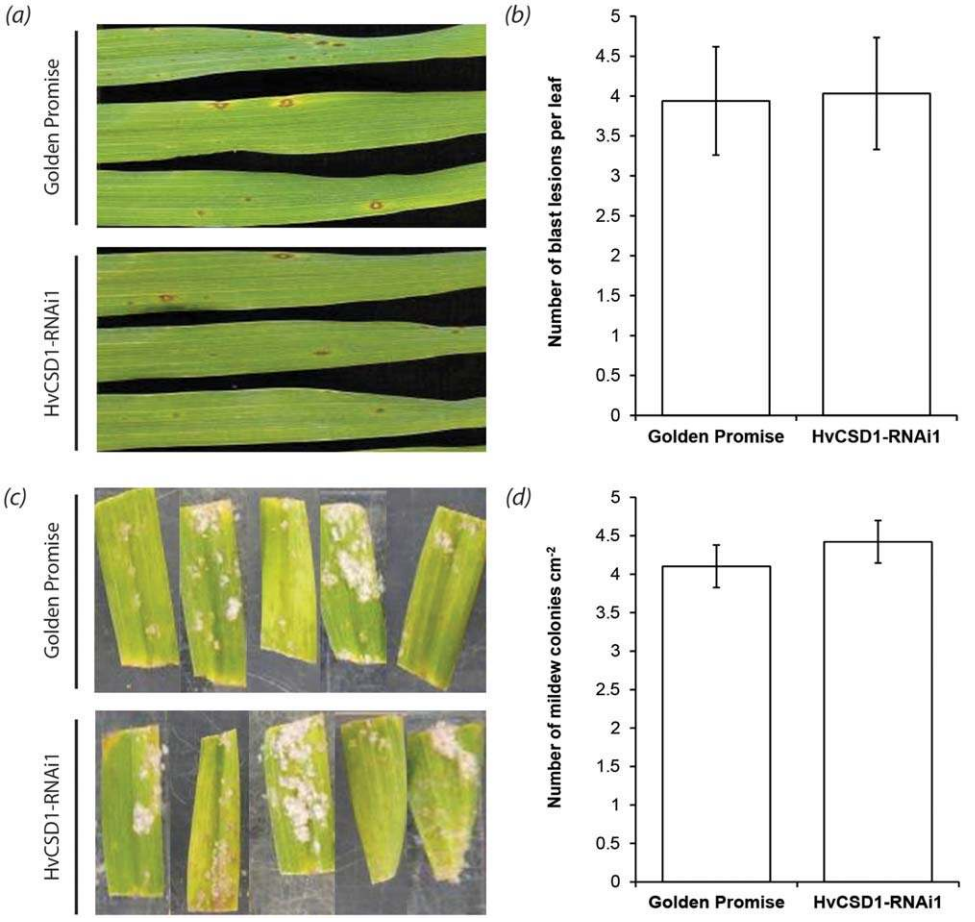

Fig. 5 Effect of *HvCSD1* silencing on the development of disease symptoms caused by *Magnaporthe oryzae* (a, b) and *Blumeria graminis* f. sp. *hordei* (c, d) on barley leaves. Blast disease symptoms (a) and number of blast lesions per leaf (b) were determined on the second youngest leaf at 144 h post-inoculation (hpi). Representative images and data shown [means ± standard error (SE)] are for $n = 30$ across two independent experiments. Powdery mildew disease symptoms (c) and number of mildew colonies/cm^2 (d) were determined on the detached prophyll leaf at 14 days post-inoculation. Representative images and data shown (means ± SE) are for $n = 64$ across three independent experiments.

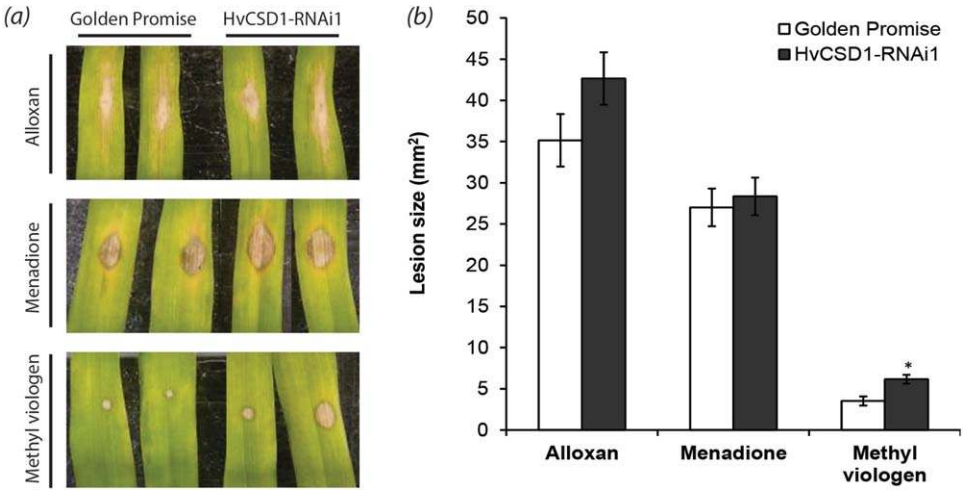

Fig. 6 Effect of *HvCSD1* silencing on reactive oxygen species (ROS)-induced lesion formation. ROS-related symptoms (a) and mean lesion size (mm) (b) were determined on the detached prophyll leaf of the wild-type barley cv. Golden Promise and HvCSD1-RNAi1 at 96 h after treatment with a ROS donor (200 mM alloxan, 100 mM menadione or 25 μM methyl viologen). Representative images and data shown [means ± standard error (SE)] are for $n = 24$ across three independent experiments. *Significant difference ($P < 0.05$) between the wild-type and HvCSD1-RNAi1 within a treatment.

only produces ROS at significant levels (Able, 2003; Liu *et al.*, 2015), but also produces necrosis-inducing effectors (Ismail *et al.*, 2014a; Liu *et al.*, 2015; Sarpeleh *et al.*, 2007, 2008), including a xylanase which appears to be necessary for the development of barley net blotch disease (Ismail *et al.*, 2014b). Furthermore, its growth pattern suggests that *Ptt* does not become necrotrophic until after 48 h (Lightfoot and Able, 2010), with most effectors and toxins being produced in the greatest quantities after this time (Ismail *et al.*, 2014b; I. Ismail and A. Able, unpublished data). Previous research in this interaction has suggested that $O_2^{\cdot-}$/$HO_2^{\cdot}$ removal might be important during resistance responses (Able, 2003). In this study, a 181-bp fragment previously identified using SSH as being up-regulated during resistance to *P. teres* (Bogacki *et al.*, 2008) was used to isolate *HvCSD1*, to characterize its expression during the plant–pathogen interaction and to predict its role through the use of knockdown lines. These lines were also used to establish that *HvCSD1* appeared to play a limited or no role in the extent of disease development on barley caused by *M. oryzae* and *Bgh*. *HvCSD1* also appeared to contribute to the regulation of ROS provided by the chloroplastic superoxide donor methyl viologen.

HvCSD1 was characterized as a 152-amino-acid cytosolic CuZnSOD (Fig. 1), constitutively expressed in all barley tissues (Fig. 2). Although cytosolic CuZnSOD is usually constitutively expressed (Kliebenstein *et al.*, 1998; Kwon and An, 2006), it can still be responsive to a range of stresses and treatments (Alscher *et al.*, 2002; Kwon and An, 2006). *HvCSD1* gene expression was increased in both susceptible and resistance responses of barley to *Ptt*, especially in the later necrotrophic stages, but to a greater extent in the resistance response (Fig. 3). CuZnSOD activity was also greater during the resistance response (Fig. 4). Similar observations for SOD activity have been made during various interactions with pathogens regarded as necrotrophic or hemi-biotrophic (Ding *et al.*, 2011; Jindřichová *et al.*, 2011; Taheri *et al.*, 2014; Wang *et al.*, 2015). These observations suggest that an increase in SOD is necessary to maintain redox status in response to pathogen attack. The observation that the removal of $O_2^{\cdot-}$/$HO_2^{\cdot}$ with exogenous ROS scavengers partially reduced cell death and symptom development in the susceptible response to *Ptt* (Able, 2003) also supports an important role for the inability to maintain redox status in the outcome of this interaction. We therefore expected that the knockdown of *HvCSD1* in the net blotch-susceptible cv. Golden Promise would facilitate symptom development during *Ptt* infection. However, disease severity was less in the knockdown lines, but still greater than that observed in the resistance response (Fig. 4). Despite the knockdown of the *HvCSD1* transcript level to as little as ~20% of wild-type expression in the RNAi lines, *HvCSD1* gene expression was induced in the knockdown lines during the interaction to a slightly greater extent than that in the susceptible cultivar early in the interaction. The apparent correlation between *HvCSD1* expression levels and disease severity suggests that HvCSD1 could contribute to the lack of cell death and symptom development observed in the resistance responses of barley to *Ptt*. However, although CuZnSOD activity was induced in the RNAi lines, this induction was unexpectedly less than in the susceptible responses. Given the complexity of ROS metabolism (Mittler *et al.*, 2004) and its overlap with other signalling pathways during plant–pathogen interactions (O'Brien *et al.*, 2012), further investigation of the impact of HvCSD1 knockdown on other elements of ROS metabolism and signalling is necessary.

Ptt development was also slower in the *HvCSD1* knockdown lines than in the susceptible cultivar, suggesting that increased levels of $O_2^{\cdot-}$/$HO_2^{\cdot}$ might impact the growth of the fungus. In the susceptible cultivar, the leaves had collapsed by 168 hpi, and the fungus was sporulating and had spread throughout the entire tissue. Most fungal growth and cell death occurred after 96 hpi. However, in the knockdown lines, the fungal growth after 96 h was much slower and, by 168 hpi, some cell death was evident near the hyphae, which had only just started to spread into the mesophyll. The pathogen may therefore be more sensitive to plant-produced $O_2^{\cdot-}$/$HO_2^{\cdot}$ during the stages that lead to sporulation. Observations in other pathosystems that fungal antioxidant gene expression increases when plant-produced ROS levels are likely to be at their highest (Keon *et al.*, 2007), such as during necrotrophic stages of the interaction and when reproductive structures are forming (Keon *et al.*, 2005, 2007), as well as the observation that virulence is lessened if the pathogen does not possess appropriate antioxidant mechanisms (Veluchamy *et al.*, 2012), support this assumption.

However, in some pathosystems, there appears to be no evidence of *in planta* oxidative stress for fungi, and fungal growth continues, regardless of the levels of plant-generated ROS, especially H_2O_2 (Samalova *et al.*, 2014; Shetty *et al.*, 2003, 2007; Temme and Tudzynski, 2009). $O_2^{\cdot-}$/$HO_2^{\cdot}$ and H_2O_2 levels were limited during the early stages of the susceptible response of barley to *Ptt*, but increased during necrosis development and just before sporulation occurred (Able, 2003). Infiltration of barley leaves with ROS scavengers also had no effect on the growth of *Ptt in planta*, suggesting that it can cope with increased levels of ROS. The slowing of fungal growth in the knockdown lines could therefore be an indirect effect of the change to the redox status on other elements of the plant–pathogen interaction, such as fungal development (Dirschnabel *et al.*, 2014; Georgiou *et al.*, 2006; Scott and Eaton, 2008; Tudzynski *et al.*, 2012), allowing the induction of the defence response (Pieterse *et al.*, 2009), especially during the early stages before the switch to necrotrophy. *HvCSD1* expression is not affected in barley lesion mimic mutants compromised in their redox status (McGrann *et al.*, 2015b), suggesting that the pathway through which *HvCSD1* maintains redox balance

is currently unknown. Given that *HvCSD1* expression and CuZnSOD activity were increased during the resistance response (Fig. 4), if overexpression of *HvCSD1* decreased disease severity, then the mechanism by which disease severity is lessened will probably be different from that in the *HvCSD1* knockdown lines. Indeed, our results might therefore reflect the potentially different roles and balance of each individual ROS ($O_2^{\cdot-}$/$HO_2^{\cdot}$ versus H_2O_2) during the different stages of growth of the fungus. Determining whether (and how) overexpression of *HvCSD1* affects the barley–*Ptt* interaction could therefore provide further insights.

Whether ROS production is modulated by toxin production during the necrotrophic stage also needs to be considered. Toxins from necrotrophs, such as *Cochliobolus sativus*, *B. cinerea* and *Fusarium* spp., induce H_2O_2 accumulation in susceptible hosts (Desmond *et al.*, 2008; Kumar *et al.*, 2001; Zhang *et al.*, 2015). The timing and extent of H_2O_2 production, fungal growth and cell death are diverse among interactions between *C. sativus* and genotypes of wheat with different resistance and susceptibility (Rodríguez-Decuadro *et al.*, 2014). A similar situation exists for *Ptt*, where isolates with different virulence have different growth habits on susceptible barley cultivars (Ismail *et al.*, 2014a), but there is no clear correlation between virulence and ROS production (Able, 2003) or between virulence and the capability to produce toxins that induce necrosis in susceptible barley cultivars (Ismail *et al.*, 2014a).

Because of these complex associations between fungal growth, toxin production, virulence and ROS production in the interaction between barley and the hemi-biotroph *Ptt*, we also investigated whether the knockdown of *HvCSD1* would affect the interaction of the susceptible cv. Golden Promise with the facultative pathogen *M. oryzae* and the obligate barley powdery mildew pathogen *Bgh*. Knockdown of *HvCSD1* had no effect on the development of disease symptoms caused by either of these pathogens (Fig. 5). ROS have been shown to increase substantially during the resistance response of barley to *Bgh*, but H_2O_2, rather than $O_2^{\cdot-}$/$HO_2^{\cdot}$, is more likely to play a role in HR and papillae formation (Hückelhoven and Kogel, 1998; Hückelhoven *et al.*, 1999). Knockdown of the respiratory burst oxidase *HvRBOHF2* did not affect HR-related cell death, but enhanced susceptibility to penetration by virulent *Bgh* in barley (Proels *et al.*, 2010), suggesting that plasma membrane-associated $O_2^{\cdot-}$/$HO_2^{\cdot}$ could also contribute to penetration resistance, even though H_2O_2 was still observed where papillae and cell wall appositions were formed. However, the application of H_2O_2 to barley prior to infection by *Bgh* prevents disease (Hafez and Király, 2003). Resistance in rice to *M. oryzae* also seems to be specifically associated with H_2O_2 and penetration resistance (Huang *et al.*, 2011). Knockdown of cytosolic *HvCSD1* would potentially lead to an increase in $O_2^{\cdot-}$/$HO_2^{\cdot}$, and not necessarily biologically significant changes in H_2O_2, and, as observed, was therefore unlikely to have an effect. Furthermore, the observations that whole barley leaf SOD activity did not change after inoculation with virulent and avirulent *Bgh* (Vanacker *et al.*, 1998), and that minimal induction of SOD activity was observed in compatible and incompatible interactions of rice with *M. oryzae* (Matsuyama, 1983), suggest that $O_2^{\cdot-}$/$HO_2^{\cdot}$ and/or HvCSD1 are unlikely to play an important role in the susceptible response of barley to *Bgh* or *M. oryzae*.

HvCSD1 knockdown also significantly increased lesion formation caused by the application of the chloroplastic $O_2^{\cdot-}$/$HO_2^{\cdot}$ donor methyl viologen at 25 μM (Fig. 6). Over-expressed chloroplastic CuZnSOD has been shown to have a protective effect, but only at low concentrations of methyl viologen (<2 μM) (Gupta *et al.*, 1993). Cytosolic CuZnSODs, such as HvCSD1, usually help the plant cell deal with general stresses and/or overflow from the mitochondrial and chloroplastic $O_2^{\cdot-}$/$HO_2^{\cdot}$ generation (Alscher *et al.*, 2002; Kwon and An, 2006). The role played by HvCSD1 in limiting lesion formation in the presence of the high concentration of methyl viologen further highlights the role of this gene in maintaining redox status, and indicates that ROS produced in excess in the chloroplast are usually propagated out into the cytosol to influence its redox state (Lee and Jo, 2004).

The cytosolic CuZnSOD *HvCSD1* contributes to the response of barley to the hemi-biotroph *Ptt*, but does not appear to play a role in the susceptible response to the hemi-biotroph *M. oryzae* or the biotroph *Bgh*. These differences mostly reflect the complex interactions between the timing of plant redox status changes and the life cycle stages for each pathogen. Where and which ROS is central to the induction of resistance or linked to symptom development, particularly cell death, also appears to be important. The observation that the removal of *HvCSD1* did not affect the susceptibility to *M. oryzae* or *Bgh*, but increased resistance to *Ptt* and slowed growth of the pathogen, therefore confirms the differential role played by H_2O_2 in different plant–pathogen interactions and suggests that $O_2^{\cdot-}$/$HO_2^{\cdot}$ contributes to the signalling responsible for the induction of resistance. Because the induction of resistance to *Ptt* in the knockdown lines was not complete, other antioxidants and/or enzymes not regulated by redox status could also contribute to the defence response and should therefore be examined in further research. However, the ability of a plant to respond appropriately to maintain or utilize redox status to control cell death appears to be an important determinant in the differential regulation of responses to pathogens with different lifestyles.

EXPERIMENTAL PROCEDURES

Plant material

Barley (*Hordeum vulgare* L.) cultivar Golden Promise, the barley breeding line CI9214, transgenic barley lines (described in more detail later) and tobacco (*Nicotiana benthamiana*) plants were grown under a 16 h day/8 h

night photoperiod at 18–21°C/12–15°C supplemented with 220–250 μmol/m^2/s fluorescent lighting in controlled environment growth rooms.

Isolation and sequence analysis of HvCSD1

A 181-bp fragment of *HvCSD1* was previously identified in an SSH screen as being up-regulated in resistant barley plants compared with susceptible plants inoculated with *P. teres* (Bogacki *et al.*, 2008). This fragment was part of the 3′ UTR and contained the start of a poly-A tail. The full-length coding sequence of *HvCSD1* was identified by locating and assembling overlapping publicly available expressed sequence tag (EST) sequences that corresponded to *HvCSD1*. The putative full-length *HvCSD1* cDNA clone was isolated by primary and nested PCR using primer pair 1 (forward, 5′-ATGGTGAAGGCTGTAGCTGTGCTT-3′; reverse, 5′-TTAGCCCTGGAGCCCGATGAT-3′) and primer pair 2 (forward, 5′-ACCGGCAGCG AGGGTGTC-3′; reverse, 5′-CCCGCAAGCAACGCGCG-3′), respectively. cDNA was synthesized from RNA extracted from the leaves of 10-day-old CI9214 seedlings using TRIZOL Reagent (Invitrogen, Carlsbad, CA, USA) with the SMART™ PCR cDNA Synthesis Kit (BD Biosciences, Clontech, Palo Alto, CA, USA) according to the manufacturer's instructions. 5′- and 3′-rapid amplification of cDNA ends (RACE) (GeneRacer Kit, Invitrogen) was performed on CI9214 cDNA according to the manufacturer's instructions to obtain the full-length *HvCSD1* mRNA. The two forward primers from primer pairs 1 and 2 were used for 3′-RACE and the two reverse primers were used for 5′-RACE. The full-length mRNA was also confirmed in cv. Sloop (Fig. S3, see Supporting Information). The *HvCSD1* genomic region encompassing the coding region of the *HvCSD1* mRNA was amplified using primer pair 1 using Sloop genomic DNA, extracted as described previously (Lightfoot *et al.*, 2008).

The full-length coding region of *HvCSD1* was used in TBLASTN searches to identify highly similar CuZnSOD sequences for evolutionary analysis. Sequences were aligned using CLUSTALW with the IUB DNA weight matrix employing a gap opening penalty of 10 and a gap extension penalty of 5. Nucleotide trees were constructed using the neighbour-joining method and the p-distance model in the Molecular Evolutionary Genetics Program (MEGA) according to Khoo *et al.* (2012). The accession numbers of the nucleotide sequences used were as follows: NM_001112234 (*ZmSOD4*), U34727 (*ZmSOD9*), NM_001056653 (*OsCuZn1*), NM_001111865 (*ZmSOD2*), AK243377 (*OsCuZn2*), NM_100757 (*AtCSD1*), AI727694 (*GhCSD1*), AJ002604 (Pship-*SOD*), AF034832 (*McSOD2*), NM_121815 (*AtCSD3*), EU597270 (*GhCSD3*), FJ393058 (*PthipI-SODC1*), AJ278671 (*PthipI-SOD1*), AJ278670 (*Pthip-SOD2*), AY566699 (*ClCuZnSODII*), EU597268 (*GhCSD2a*), NM_128379 (*AtCSD2*), NM_001069049 (*OsSODcp*), EU408345 (*ZmEU408345*), AK248474 (*HvAK248474*), U69536 (*TaSOD1*.1), U69632 (*TaSOD1*.2) and U51242 (*EcSODC*). Sequences were analysed using Vector NTI version 10 (Invitrogen) and Genedoc version 2.6.002 (http://www.nrbsc.org/gfx/genedoc). The intron and exon structures of the genes corresponding to the transcripts used in the phylogenetic analysis were determined when the genomic and mRNA sequence data were available. The full-length CDS for Sloop and CI9214 and the nucleotide sequence for the *HvCSD1* gene in Sloop were submitted to the GenBank database under accession numbers KU179439, KU179438 and KU179440, respectively.

Subcellular localization of HvCSD1

The full-length coding region of *HvCSD1* was amplified from CI9214 genomic DNA (using the primers 5′-CACCATGGTGAAGGCTGTAGC TGTGCTT-3′ and 5′-GCCCTGGAGCCCGATGAT-3′) and cloned into the pCR8 entry vector (Invitrogen). *HvCSD1* was then transferred into the pMDC83 binary vector (Curtis and Grossniklaus, 2003) using LR Clonase™ Plus Enzyme Mix (Invitrogen) according to the manufacturer's instructions. The *35S::HvCSD1-GFP* fusion construct was introduced into *Agrobacterium tumefaciens* (strain AGL1) following the method of An *et al.* (1989) and *N. benthamiana* leaves were infiltrated as described previously (Selth *et al.*, 2004). Plant tissue was sampled after 3 days and analysed for GFP expression with an SP5 spectral scanning confocal microscope (Leica Microsystems, Wetzlar, Germany), using an excitation wavelength of 488 nm. *Z*-step image collection occurred from the top to the bottom of the leaves at 1-μm intervals and *Z*-stack images were prepared using Confocal Assistant (version 4.02, Todd Clark Brelje, MN, USA). pMDC83 without the *HvCSD1* insert was used as a control for GFP localization. Subcellular localization occurred in three independent experiments.

Production of HvCSD1-RNAi knockdown lines in barley

A 172-bp region of the *HvCSD1* 3′ UTR was amplified from cDNA from CI9214 with the 5′-CACCACAGATCTTGGCACTTGAAGG-3′ and 5′-GACAGAACTGAACTGTTCCAGTCACG-3′ primers, and cloned into the pENTR/D-TOPO® vector (Invitrogen) according to the manufacturer's instructions. The specificity of knockdown to *HvCSD1* was confirmed as follows: BLAST analysis of the barley genome assembly (GCA_000326085.1) using EnsemblPlants (plants.ensembl.org); alignment with *HvCSD1* and the two other CSDs identified in the barley genome (MLOC_17760, previously characterized as *HvSOD1*, a chloroplastic CSD, and MLOC_38479, a peroxisomal CSD or *HvCSD3*); and detection of RNAi targets of loci identified in the BLAST analysis and the CSDs with siFi (version 3.2, Snowformatics). The 172-bp region was specific to *HvCSD1* (Fig. S4, Table S2, see Supporting Information) and was predicted to be specific to *HvCSD1* with 54 effective hits (of 152 total hits). The 172-bp cassette was transferred into the hairpin RNAi vector pSTARGATE (Wesley *et al.*, 2001) using LR Clonase™ Plus Enzyme Mix (Invitrogen) according to the manufacturer's instructions. The resultant vector was utilized in *Agrobacterium*-mediated transformation of barley cv. Golden Promise, and putative transformants were screened according to previously established methods (Lloyd *et al.*, 2007). Putatively transformed plants were screened at the T_1 generation for the presence of the hygromycin resistance gene by PCR with the primers 5′-CTTTGCCCTCGGACGAGTGCTGGGGC-3′ and 5′-TGAACTCACCGCGACGTCTGTCGA-3′ under the following conditions: 94°C for 5 min, 25 cycles of 94°C for 30 s, 60°C for 30 s, 72°C for 90 s, and a final extension step of 72°C for 7 min. At the T_2 generation, lines positive for the hygromycin resistance gene were screened for homozygotes and transgene insertion number by Southern analysis with 20 μg of genomic DNA digested with *Eco*RV or *Hin*dIII (New England Biolabs, Beverly, MA, USA). The Southern blots were screened with a fragment of the hygromycin resistance gene amplified using the primers listed above (Fig. S1). HvCSD1-RNAi1 and HvCSD1-RNAi2 are lines created from independent transformation events and both contain one copy of the transgene.

HvCSD1 gene expression

RT-PCR was initially used to confirm the extent of knockdown in the transgenic lines. RT-PCR was also used to determine *HvCSD1* gene expression in a tissue series from cv. Golden Promise and during the barley–*Ptt* interaction. RNA for the analysis of *HvCSD1* abundance in the transgenic lines was prepared from the second leaves of 3-week-old plants using TRIZOL Reagent according to the manufacturer's instructions. For the analysis of *HvCSD1* abundance in different Golden Promise tissue types, RNA was prepared from the first leaves of 3-week-old plants, from flag leaves and immature heads of 18-week-old plants, and from roots and coleoptiles of 7-day-old seedlings grown in 24-well microplates (Iwaki Glass Co., Funahashi, Japan) at 22°C in the dark. For the interaction between barley and *Ptt*, RNA was prepared from the second leaves of inoculated and mock-inoculated control plants at multiple time points during the interaction. All RT-PCR experiments were performed on at least three biologically distinct samples.

RT-PCR was performed using the SuperScript One-Step RT-PCR kit from Invitrogen according to the manufacturer's instructions with the primers 5′-ACCGCACTTCAACCCCGCTGGTCATGTG-3′ and 5′-GAGCCCGATGATCCCGCAAGCAACACGC-3′. RNA (100 ng) was used as template in each reaction: 50°C for 30 min, 94°C for 2 min, 32 cycles of 94°C for 30 s, 60°C for 30 s, 72°C for 1 min, and a final extension step of 72°C for 10 min. To monitor RNA loading, a region of *H. vulgare glyceraldehyde-3-phosphate dehydrogenase* (*HvGAPDH*), considered to be an ideal reference gene in barley (Jarosova and Kundu, 2010), was amplified from the same RNA samples under the same conditions using the primers 5′-GTGAGGCTGGTGCTGATTACG-3′ and 5′-TGGTGCAGCTAGCATTTGAGAC-3′. Knockdown of expression in the *HvCSD1*-RNAi1 line was further confirmed in 14-day-old prophyll leaves using qRT-PCR, with *HvCSD1* transcript levels assessed using gene-specific primers (forward, 5′-ACCTCGGAAATGTGACAGC-3′; reverse, 5′-ACCCTTGCCAAGATCATCAG-3′), as described previously (McGrann *et al.*, 2015a; Tufan *et al.*, 2009).

SOD protein activity

Total protein was prepared from at least three biologically distinct samples, as described by Van Camp *et al.* (1994), and checked by separation on 12% denaturing sodium dodecyl sulfate-polyacrylamide gel electrophoresis (SDS-PAGE) gels using Coomassie staining (Wang *et al.*, 2007). To identify bands of SOD activity, 100 μg of total protein were run on 12% non-denaturing polyacrylamide gels and subsequently stained for SOD activity as described previously (Beauchamp and Fridovich, 1971), except for the use of a reduced nitroblue tetrazolium concentration of 1 mM. Different SOD isoenzyme activities were determined by differential inhibition (Fridovich, 1975) by soaking the gels in 3 mM H_2O_2 or 3 mM KCN for 20 min prior to gel illumination.

Barley–*Ptt* interaction

Barley plants at Zadoks' growth stage 14 (Zadoks *et al.*, 1974) were inoculated with 20 000 spores/mL (in 0.1% v/v Tween-20) of *Ptt* isolate NB50 (kindly provided by Hugh Wallwork, South Australian Research and Development Institute, Urrbrae, South Australia, Australia) using an atomizer (Preval, Yonkers, NY, USA), as described previously (Lightfoot and Able, 2010). Symptoms of *Ptt* infection on second leaves were scored for the percentage of leaf area affected by necrosis and chlorosis using a scale of 0–5 (0, 0%; 1, 1%–10%; 2, 11%–25%; 3, 26%–50%; 4, 51%–75%; 5, 76%–100%). Images were also taken of the leaves using a CanoScan 5600F scanner (Canon, Tokyo, Japan). To visualize and assess fungal growth and development, microscopic analysis assessed 10 germinated conidia on each of five cleared leaves using a 0–10 numerical scale that rates the development of *Ptt* during the interaction *in planta* (Lightfoot and Able, 2010). Data from two independent inoculation experiments were analysed with GenStat 11 (Lawes Agricultural Trust, VSN International Ltd., Hemel Hempstead, Hertfordshire, UK) using analysis of variance (ANOVA). The least-significant difference (l.s.d.) at $P = 0.05$ was used to determine significant differences between means.

Barley–*M. oryzae* interaction

Plants at growth stage 13 (Zadoks *et al.*, 1974) were spray inoculated with 100 000 spores/mL of *M. oryzae* isolate BR32 as described previously (Tufan *et al.*, 2009). Disease development was assessed by the number of blast lesions visible on the second leaf of each plant at 6 days post-inoculation (dpi) from two independent inoculation experiments (for a total of 30 leaves). Data were analysed in GenStat15 using general linear modelling that took into account variation caused by the different lines and experiments.

Barley–*Bgh* inoculation

Detached prophyll leaves from 14-day-old plants were cut into approximately 2-cm-long segments, placed into clear plastic boxes containing 0.5% water agar supplemented with 100 mg/L benzimidazole and inoculated with *Bgh* isolate CC148 following the method of Boyd *et al.* (1994). Pathogen infection was assessed as the number of colonies observed per square centimetre of leaf area from three independent inoculation experiments, each consisting of a minimum of eight replicate leaves of each line. Data were analysed in GenStat15 using general linear modelling that took into account the variation caused by the different lines and experiments.

ROS induction of cell death by pharmacological agents

The H_2O_2 donor alloxan, the mitochondrial $O_2^{\cdot-}/HO_2^{\cdot}$ donor menadione and the chloroplastic $O_2^{\cdot-}/HO_2^{\cdot}$ donor methyl viologen were used to induce cell death in detached prophyll leaves according to McGrann *et al.* (2015a). ROS-induced lesion size was measured from photographs of each box taken 96 h after ROS donor treatment using ImageJ (Abràmoff *et al.*, 2004). Data for each ROS donor were analysed in GenStat15 using general linear modelling that took into account the variation caused by the different lines and experiments.

ACKNOWLEDGEMENTS

This work was partially funded by the Grains Research and Development Corporation (CMB0009) and the Molecular Plant Breeding Cooperative Research Centre. GRDM was supported by the Biotechnology and Biological Sciences Research Council (BBSRC) Biotic Interactions Strategic Programme grant reference BBJ004553/1. Thanks are due to Rohan Singh, Alan Little and Nigel Percy for technical assistance with the development

of the knockdown lines, GFP localization and SOD activity assays, respectively. The authors have no conflicts of interest to declare.

REFERENCES

Able, A.J. (2003) Role of reactive oxygen species in the response of barley to necrotrophic pathogens. *Protoplasma*, **221**, 137–143.

Able, A.J., Guest, D.I. and Sutherland, M.W. (1998) Use of a new tetrazolium-based assay to study the production of superoxide radicals by tobacco cell cultures challenged with avirulent zoospores of *Phytophthora parasitica* var *nicotianae*. *Plant Physiol.* **117**, 491–499.

Able, A.J., Guest, D.I. and Sutherland, M.W. (2000) Hydrogen peroxide yields during the incompatible interaction of tobacco suspension cells inoculated with *Phytophthora nicotianae*. *Plant Physiol.* **124**, 899–910.

Abràmoff, M.D., Magalhães, P.J. and Ram, S.J. (2004) Image processing with ImageJ. *Biophoton. Int.* **11**, 36–42.

Alscher, R.G., Erturk, N. and Heath, L.S. (2002) Role of superoxide dismutases (SODs) in controlling oxidative stress in plants. *J. Exp. Bot.* **53**, 1331–1341.

An, G., Ebert, P., Mitra, A. and Ha, S. (1989) Binary vectors. In: *Plant Molecular Biology Manual* (**Gelvin, S.**, **Schilperoort, R.** and **Verma, D.**, eds), pp. 1–19. Dordrecht: Springer.

Asada, K., Kiso, K. and Yoshikawa, K. (1974) Univalent reduction of molecular oxygen by spinach chloroplasts on illumination. *J. Biol. Chem.* **249**, 2175–2181.

Barna, B., Fodor, J., Harrach, B., Pogány, M. and Király, Z. (2012) The Janus face of reactive oxygen species in resistance and susceptibility of plants to necrotrophic and biotrophic pathogens. *Plant Physiol. Biochem.* **59**, 37–43.

Baxter, A., Mittler, R. and Suzuki, N. (2014) ROS as key players in plant stress signalling. *J. Exp. Bot.* **65**, 1229–1240.

Beauchamp, C. and Fridovich, I. (1971) Superoxide dismutase: improved assays and an assay applicable to acrylamide gels. *Anal. Biochem.* **44**, 276–287.

Blokhina, O., Virolainen, E. and Fagerstedt, K.V. (2003) Antioxidants, oxidative damage and oxygen deprivation stress: a review. *Ann. Bot.* **91**, 179–194.

Bogacki, P., Oldach, K.H. and Williams, K.J. (2008) Expression profiling and mapping of defence response genes associated with the barley–*Pyrenophora teres* incompatible interaction. *Mol. Plant Pathol.* **9**, 645–660.

Bowler, C., Van Camp, W., Van Montagu, M., Inzé, D. and Asada, K. (1994) Superoxide dismutase in plants. *Crit. Rev. Plant Sci.* **13**, 199–218.

Boyd, L.A., Smith, P.H., Green, R.M. and Brown, J.K. (1994) The relationship between the expression of defense-related genes and mildew development in barley. *Mol. Plant–Microbe Interact.* **7**, 401–410.

Conklin, P.L. and Last, R.L. (1995) Differential accumulation of antioxidant mRNAs in *Arabidopsis thaliana* exposed to ozone. *Plant Physiol.* **109**, 203–212.

Curtis, M.D. and Grossniklaus, U. (2003) A gateway cloning vector set for high-throughput functional analysis of genes in planta. *Plant Physiol.* **133**, 462–469.

Dat, J., Vandenabeele, S., Vranová, E., Van Montagu, M., Inzé, D. and Van Breusegem, F. (2002) Dual action of the active oxygen species during plant stress responses. *Cell. Mol. Life Sci.* **57**, 779–795.

Delledonne, M., Zeier, J., Marocco, A. and Lamb, C. (2001) Signal interactions between nitric oxide and reactive oxygen intermediates in the plant hypersensitive disease resistance response. *Proc. Natl. Acad. Sci. USA*, **98**, 13 454–13 459.

Desmond, O.J., Manners, J.M., Stephens, A.E., Maclean, D.J., Schenk, P.M., Gardiner, D.M., Munn, A.L. and Kazan, K. (2008) The Fusarium mycotoxin deoxynivalenol elicits hydrogen peroxide production, programmed cell death and defence responses in wheat. *Mol. Plant Pathol.* **9**, 435–445.

Ding, L., Xu, H., Yi, H., Yang, L., Kong, Z., Zhang, L., Xue, S., Jia, H. and Ma, Z. (2011) Resistance to hemi-biotrophic *F. graminearum* infection is associated with coordinated and ordered expression of diverse defense signaling pathways. *PLoS One*, **6**, e19008.

Dirschnabel, D.E., Nowrousian, M., Cano-Domínguez, N., Aguirre, J., Teichert, I. and Kück, U. (2014) New insights into the roles of NADPH oxidases in sexual development and ascospore germination in *Sordaria macrospora*. *Genetics*, **196**, 729–744.

Frederickson Matika, D.E. and Loake, G.J. (2014) Redox regulation in plant immune function. *Antioxid. Redox Signal.* **21**, 1373–1388.

Fridovich, I. (1975) Superoxide dismutases. *Annu. Rev. Biochem.* **44**, 147–159.

Gadjev, I., Stone, J.M. and Gechev, T.S. (2008) Chapter 3: programmed cell death in plants: new insights into redox regulation and the role of hydrogen peroxide. In: *International Review of Cell and Molecular Biology*, (Jeon, K.W., ed), 270, 87–144. San Diego: Academic Press.

Georgiou, C.D., Patsoukis, N., Papapostolou, I. and Zervoudakis, G. (2006) Sclerotial metamorphosis in filamentous fungi is induced by oxidative stress. *Integr. Comp. Biol.* **46**, 691–712.

Govrin, E.M. and Levine, A. (2000) The hypersensitive response facilitates plant infection by the necrotrophic pathogen *Botrytis cinerea*. *Curr. Biol.* **10**, 751–757.

Groß, F., Durner, J. and Gaupels, F. (2013) Nitric oxide, antioxidants and prooxidants in plant defence responses. *Front. Plant Sci.* **4, 419**.

Gupta, A.S., Heinen, J.L., Holaday, A.S., Burke, J.J. and Allen, R.D. (1993) Increased resistance to oxidative stress in transgenic plants that overexpress chloroplastic Cu/Zn superoxide dismutase. *Proc. Natl. Acad. Sci. USA*, **90**, 1629–1633.

Hafez, Y.M. and Király, Z. (2003) Role of hydrogen peroxide in symptom expression of barley susceptible and resistant to powdery mildew. *Acta Phytopathol. Entomol. Hung.* **38**, 227–236.

Heller, J. and Tudzynski, P. (2011) Reactive oxygen species in phytopathogenic fungi: signaling, development, and disease. *Annu. Rev. Phytopathol.* **49**, 369–390.

Huang, K., Czymmek, K.J., Caplan, J.L., Sweigard, J.A. and Donofrio, N.M. (2011) Suppression of plant-generated reactive oxygen species is required for successful infection by the rice blast fungus. *Virulence*, **2**, 559–562.

Hückelhoven, R. and Kogel, K.-H. (1998) Tissue-specific superoxide generation at interaction sites in resistant and susceptible near-isogenic barley lines attacked by the powdery mildew fungus (*Erysiphe graminis* f. sp. *hordei*). *Mol. Plant–Microbe Interact.* **11**, 292–300.

Hückelhoven, R., Fodor, J., Preis, C. and Kogel, K.-H. (1999) Hypersensitive cell death and papilla formation in barley attacked by the powdery mildew fungus are associated with hydrogen peroxide but not with salicylic acid accumulation. *Plant Physiol.* **119**, 1251–1260.

Ismail, I., Godfrey, D. and Able, A. (2014a) Fungal growth, proteinaceous toxins and virulence of *Pyrenophora teres* f. *teres* on barley. *Australas. Plant Pathol.* **43**, 535–546.

Ismail, I., Godfrey, D. and Able, A. (2014b) Proteomic analysis reveals the potential involvement of xylanase from *Pyrenophora teres* f. *teres* in net form net blotch disease of barley. *Australas. Plant Pathol.* **43**, 715–726.

Jarosova, J. and Kundu, J.K. (2010) Validation of reference genes as internal control for studying viral infections in cereals by quantitative real-time RT-PCR. *BMC Plant Biol.* **10**, 9.

Jindřichová, B., Fodor, J., Šindelářová, M., Burketová, L. and Valentová, O. (2011) Role of hydrogen peroxide and antioxidant enzymes in the interaction between a hemibiotrophic fungal pathogen, *Leptosphaeria maculans*, and oilseed rape. *Environ. Exp. Bot.* **72**, 149–156.

Keon, J., Rudd, J.J., Antoniw, J., Skinner, W., Hargreaves, J. and Hammond-Kosack, K. (2005) Metabolic and stress adaptation by *Mycosphaerella graminicola* during sporulation in its host revealed through microarray transcription profiling. *Mol. Plant Pathol.* **6**, 527–540.

Keon, J., Antoniw, J., Carzaniga, R., Deller, S., Ward, J.L., Baker, J.M., Beale, M.H., Hammond-Kosack, K. and Rudd, J.J. (2007) Transcriptional adaptation of *Mycosphaerella graminicola* to programmed cell death (PCD) of its susceptible wheat host. *Mol. Plant–Microbe Interact.* **20**, 178–193.

Khoo, K.H., Able, A.J. and Able, J.A. (2012) Poor Homologous Synapsis 1 interacts with chromatin but does not colocalise with ASYnapsis 1 during early meiosis in bread wheat. *Int. J. Plant Genomics*, **2012**, 514398.

Kliebenstein, D.J., Monde, R.-A. and Last, R.L. (1998) Superoxide dismutase in Arabidopsis: an eclectic enzyme family with disparate regulation and protein localization. *Plant Physiol.* **118**, 637–650.

Kumar, J., Hückelhoven, R., Beckhove, U., Nagarajan, S. and Kogel, K.-H. (2001) A compromised Mlo pathway affects the response of barley to the necrotrophic fungus *Bipolaris sorokiniana* (Teleomorph: *Cochliobolus sativus*) and its toxins. *Phytopathology*, **91**, 127–133.

Kwon, S.I. and An, C.S. (2006) Differential expression of two SOD (Superoxide dismutase) genes from small radish (*Rhaphanus sativus* L. var. *sativus*). *J. Plant Biol.* **49**, 477–483.

Lee, H. and Jo, J. (2004) Increased tolerance to methyl viologen by transgenic tobacco plants that over-express the cytosolic glutathione reductase gene from *Brassica campestris*. *J. Plant Biol.* **47**, 111–116.

Lehmann, S., Serrano, M., L'Haridon, F., Tjamos, S.E. and Metraux, J.-P. (2015) Reactive oxygen species and plant resistance to fungal pathogens. *Phytochemistry*, **112**, 54–62.

Levine, A., Tenhaken, R., Dixon, R. and Lamb, C. (1994) H_2O_2 from the oxidative burst orchestrates the plant hypersensitive disease resistance response. *Cell*, **79**, 583–593.

Li, C., Barker, S.J., Gilchrist, D.G., Lincoln, J.E. and Cowling, W.A. (2008a) *Leptosphaeria maculans* elicits apoptosis coincident with leaf lesion formation and hyphal advance in *Brassica napus*. *Mol. Plant–Microbe Interact.* **21**, 1143–1153.

Li, H., Sivasithamparam, K., Barbetti, M.J., Wylie, S.J. and Kuo, J. (2008b) Cytological responses in the hypersensitive reaction in cotyledon and stem tissues of *Brassica napus* after infection by *Leptosphaeria maculans*. *J. Gen. Plant Pathol.* **74**, 120–124.

Lightfoot, D.J. and Able, A.J. (2010) Growth of *Pyrenophora teres* in planta during barley net blotch disease. *Australas. Plant Pathol.* **39**, 499–507.

Lightfoot, D.J., Boettcher, A., Little, A., Shirley, N. and Able, A.J. (2008) Identification and characterisation of barley (*Hordeum vulgare*) respiratory burst oxidase homologue family members. *Funct. Plant Biol.* **35**, 347–359.

Liu, Z., Holmes, D.J., Faris, J.D., Chao, S., Brueggeman, R.S., Edwards, M.C. and Friesen, T.L. (2015) Necrotrophic effector-triggered susceptibility (NETS) underlies the barley–*Pyrenophora teres* f. *teres* interaction specific to chromosome 6H. *Mol. Plant Pathol.* **16**, 188–200.

Lloyd, A.H., Milligan, A.S., Langridge, P. and Able, J.A. (2007) TaMSH7: a cereal mismatch repair gene that affects fertility in transgenic barley (*Hordeum vulgare* L.). *BMC Plant Biol.* **7**, 67.

Lo Presti, L., Lanver, D., Schweizer, G., Tanaka, S., Liang, L., Tollot, M., Zuccaro, A., Reissmann, S. and Kahmann, R. (2015) Fungal effectors and plant susceptibility. *Annu. Rev. Plant Biol.* **66**, 513–545.

Matsuyama, N. (1983) Time course alteration of lipid peroxidation and the activities of superoxide dismutase, catalase and peroxidase in blast infected rice leaves. *Ann. Phytopathol. Soc. Jpn.* **49**, 270–273.

McGrann, G.R.D., Steed, A., Burt, C., Goddard, R., Lachaux, C., Bansal, A., Corbitt, M., Gorniak, K., Nicholson, P. and Brown, J.K. (2015a) Contribution of the drought tolerance-related stress-responsive NAC1 transcription factor to resistance of barley to *Ramularia* leaf spot. *Mol. Plant Pathol.* **16**, 201–209.

McGrann, G.R.D., Steed, A., Burt, C., Nicholson, P. and Brown, J.K.M. (2015b) Differential effects of lesion mimic mutants in barley on disease development by facultative pathogens. *J. Exp. Bot.* **66**, 3417–3428.

Miller, A.-F. (2012) Superoxide dismutases: ancient enzymes and new insights. *FEBS Lett.* **586**, 585–595.

Mittler, R., Vanderauwera, S., Gollery, M. and Van Breusegem, F. (2004) Reactive oxygen gene network of plants. *Trends Plant Sci.* **9**, 490–498.

Myouga, F., Hosoda, C., Umezawa, T., Iizumi, H., Kuromori, T., Motohashi, R., Shono, Y., Nagata, N., Ikeuchi, M. and Shinozaki, K. (2008) A heterocomplex of iron superoxide dismutases defends chloroplast nucleoids against oxidative stress and is essential for chloroplast development in Arabidopsis. *Plant Cell*, **20**, 3148–3162.

O'Brien, J.A., Daudi, A., Butt, V.S. and Bolwell, G.P. (2012) Reactive oxygen species and their role in plant defence and cell wall metabolism. *Planta*, **236**, 765–779.

Ogawa, K.I., Kanematsu, S. and Asada, K. (1996) Intra- and extra-cellular localization of "cytosolic" CuZn-superoxide dismutase in spinach leaf and hypocotyl. *Plant Cell Physiol.* **37**, 790–799.

Pastori, G.M. and Foyer, C.H. (2002) Common components, networks, and pathways of cross-tolerance to stress. The central role of "redox" and abscisic acid-mediated controls. *Plant Physiol.* **129**, 460–468.

Pieterse, C.M., Leon-Reyes, A., Van der Ent, S. and Van Wees, S.C. (2009) Networking by small-molecule hormones in plant immunity. *Nat. Chem. Biol.* **5**, 308–316.

Proels, R.H., Oberhollenser, K., Pathuri, I.P., Hensel, G., Kumlehn, J. and Hückelhoven, R. (2010) RBOHF2 of barley is required for normal development of penetration resistance to the parasitic fungus *Blumeria graminis* f. sp. *hordei*. *Mol. Plant–Microbe Interact.* **23**, 1143–1150.

Rhoads, D.M., Umbach, A.L., Subbaiah, C.C. and Siedow, J.N. (2006) Mitochondrial reactive oxygen species. Contribution to oxidative stress and interorganellar signaling. *Plant Physiol.* **141**, 357–366.

del Rio, L.A., Corpas, F.J., Sandalio, L.M., Palma, J.M. and Barroso, J.B. (2003) Plant peroxisomes, reactive oxygen metabolism and nitric oxide. *IUBMB Life*, **55**, 71–81.

Rodríguez-Decuadro, S., Silva, P., Bentancur, O., Gamba, F. and Pritsch, C. (2014) Histochemical characterization of early response to C*ochliobolus sativus* infection in selected barley genotypes. *Phytopathology*, **104**, 715–723.

Samalova, M., Meyer, A.J., Gurr, S.J. and Fricker, M.D. (2014) Robust antioxidant defences in the rice blast fungus *Magnaporthe oryzae* confer tolerance to the host oxidative burst. *New Phytol.* **201**, 556–573.

Sarpeleh, A., Wallwork, H., Catcheside, D.E., Tate, M.E. and Able, A.J. (2007) Proteinaceous metabolites from *Pyrenophora teres* contribute to symptom development of barley net blotch. *Phytopathology*, **97**, 907–915.

Sarpeleh, A., Wallwork, H., Tate, M.E., Catcheside, D.E. and Able, A.J. (2008) Initial characterisation of phytotoxic proteins isolated from *Pyrenophora teres*. *Physiol. Mol. Plant Pathol.* **72**, 73–79.

Scott, B. and Eaton, C.J. (2008) Role of reactive oxygen species in fungal cellular differentiations. *Curr. Opin. Microbiol.* **11**, 488–493.

Selth, L.A., Randles, J.W. and Rezaian, M.A. (2004) Host responses to transient expression of individual genes encoded by Tomato leaf curl virus. *Mol. Plant–Microbe Interact.* **17**, 27–33.

Shetty, N.P., Kristensen, B., Newman, M.-A., Møller, K., Gregersen, P.L. and Jørgensen, H.L. (2003) Association of hydrogen peroxide with restriction of *Septoria tritici* in resistant wheat. *Physiol. Mol. Plant Pathol.* **62**, 333–346.

Shetty, N.P., Mehrabi, R., Lütken, H., Haldrup, A., Kema, G.H., Collinge, D.B. and Jørgensen, H.J. (2007) Role of hydrogen peroxide during the interaction between the hemibiotrophic fungal pathogen *Septoria tritici* and wheat. *New Phytol.* **174**, 637–647.

Sutherland, M.W. (1991) The generation of oxygen radicals during host plant responses to infection. *Physiol. Mol. Plant Pathol.* **39**, 79–93.

Taheri, P., Irannejad, A., Goldani, M. and Tarighi, S. (2014) Oxidative burst and enzymatic antioxidant systems in rice plants during interaction with *Alternaria alternata*. *Eur. J. Plant Pathol.* **140**, 829–839.

Temme, N. and Tudzynski, P. (2009) Does *Botrytis cinerea* ignore H_2O_2-induced oxidative stress during infection? Characterization of *Botrytis* activator protein 1. *Mol. Plant–Microbe Interact.* **22**, 987–998.

Tudzynski, P., Heller, J. and Siegmund, U. (2012) Reactive oxygen species generation in fungal development and pathogenesis. *Curr. Opin. Microbiol.* **15**, 653–659.

Tufan, H.A., McGrann, G.R., Magusin, A., Morel, J.B., Miché, L. and Boyd, L.A. (2009) Wheat blast: histopathology and transcriptome reprogramming in response to adapted and non-adapted *Magnaporthe* isolates. *New Phytol.* **184**, 473–484.

Van Camp, W., Bowler, C., Villarroel, R., Tsang, E., Van Montagu, M. and Inze, D. (1990) Characterization of iron superoxide dismutase cDNAs from plants obtained by genetic complementation in *Escherichia coli*. *Proc. Natl. Acad. Sci. USA*, **87**, 9903–9907.

Van Camp, W., Willekens, H., Bowler, C., Van Montagu, M., Inzé, D., Reupold-Popp, P., Sandermann, H. and Langebartels, C. (1994) Elevated levels of superoxide dismutase protect transgenic plants against ozone damage. *Nat. Biotechnol.* **12**, 165–168.

Vanacker, H., Harbinson, J., Ruisch, J., Carver, T. and Foyer, C. (1998) Antioxidant defences of the apoplast. *Protoplasma*, **205**, 129–140.

Veluchamy, S., Williams, B., Kim, K. and Dickman, M.B. (2012) The CuZn superoxide dismutase from *Sclerotinia sclerotiorum* is involved with oxidative stress tolerance, virulence, and oxalate production. *Physiol. Mol. Plant Pathol.* **78**, 14–23.

Wang, X., Li, X. and Li, Y. (2007) A modified Coomassie Brilliant Blue staining method at nanogram sensitivity compatible with proteomic analysis. *Biotechnol. Lett.* **29**, 1599–1603.

Wang, Y., Moidu, H., Charles, M.T., Dube, C. and Khanizadeh, S. (2015) Differential regulation of superoxide dismutase activity in selected strawberry lines exposed to *Mycosphaerella fragariae*. *J. Plant Stud.* **4**, 30.

Wesley, S.V., Helliwell, C.A., Smith, N.A., Wang, M., Rouse, D.T., Liu, Q., Gooding, P.S., Singh, S.P., Abbott, D., Stoutjesdijk, P.A., Robinson, S.P., Gleave, A.P., Green, A.G. and Waterhouse, P.M. (2001) Construct design for efficient, effective and high-throughput gene silencing in plants. *Plant J.* **27**, 581–590.

Zadoks, J.C., Chang, T.T. and Konzak, C.F. (1974) A decimal code for the growth stages of cereals. *Weed Res.* **14**, 415–421.

Zhang, Y., Zhang, Y., Qiu, D., Zeng, H., Guo, L. and Yang, X. (2015) BcGs1, a glycoprotein from *Botrytis cinerea*, elicits defence response and improves disease resistance in host plants. *Biochem. Biophys. Res. Commun.* **457**, 627–634.

SUPPORTING INFORMATION

Additional Supporting Information may be found in the online version of this article at the publisher's website:

Fig. S1 Southern analysis of T2 *HvCSD1*-RNAi lines.
Fig. S2 RNAi silencing of *HvCSD1* in transgenic barley plants.
Fig. S3 Comparison of full-length coding sequences for *HvCSD1* (a) and their translation (b) for the barley breeding line CI9214 and cv. Sloop.
Fig. S4 Comparison of the 172-bp region of the 3′ untranslated region (UTR) of *HvCSD1* used in the *HvCSD1*-RNAi construct with the full-length coding sequences and 3′ UTR of other CSDs in barley.
Table S1 Exon structure of the genes used in the phylogenetic analysis (Fig. 1b).
Table S2 BLAST analysis of the barley genome assembly (GCA_000326085.1, EnsemblPlants) with the 172-bp region used in the *HvCSD1*-RNAi construct.